frontiers | Frontiers in Materials

TYPE Original Research
PUBLISHED 07 October 2022
DOI 10.3389/fmats.2022.1031538

OPEN ACCESS

EDITED BY
Chunli Zhang,
Zhejiang University, China

REVIEWED BY
Xu Liang,
Xi'an Jiaotong University, China
Zhijing Wu,
Harbin Engineering University, China

*CORRESPONDENCE
Lele Zhang,
zhangll@stdu.edu.cn

SPECIALTY SECTION
This article was submitted to Smart Materials,
a section of the journal
Frontiers in Materials

RECEIVED 30 August 2022
ACCEPTED 15 September 2022
PUBLISHED 07 October 2022

CITATION
Nie G, Lei Z, Liu J and Zhang L (2022), Bending waves localized along the edge of a semi-infinite piezoelectric plate with orthogonal symmetry.
Front. Mater. 9:1031538.
doi: 10.3389/fmats.2022.1031538

Bending waves localized along the edge of a semi-infinite piezoelectric plate with orthogonal symmetry

Guoquan Nie[1,2], Zhenyu Lei[3], Jinxi Liu[1] and Lele Zhang[1,3]*

[1]State Key Laboratory of Mechanical Behavior and System Safety of Traffic Engineering Structures, Shijiazhuang Tiedao University, Shijiazhuang, China, [2]School of Mechanical Engineering, Shijiazhuang Tiedao University, Shijiazhuang, China, [3]Department of Engineering Mechanics, Shijiazhuang Tiedao University, Shijiazhuang, China

We study the propagation of bending waves along the free edge of a semi-infinite piezoelectric plate within the framework of two-variable refined plate theory (TVPT, a high-order plate theory), Reissner-Mindlin refined plate theory (RMPT, a first-order plate theory), and the classical plate theory (CPT). The piezoelectric plate has macroscopic symmetry of orthogonal mm2 The governing equations are derived using Hamilton principle. The dispersion relations for electrically open and shorted boundary conditions at the free edge are obtained analytically. The difference in dispersion property between the three plate theories is analyzed. The numerical results show that the dispersion curves predicted by TVPT and RMPT are similar and have small difference over the complete frequency range, which means both the two theories are valid for the analysis of edge waves in a piezoelectric plate. But the wave velocity calculated by CPT is much larger than the two theories above and is no longer valid for high frequency and thick plate. The electrical boundary condition at the free edge has an insignificant effect on phase velocity and group velocity which can be ignored for the analysis of edge waves in a piezoelectric plate governed by bending deformation. The velocity of bending edge waves in a semi-infinite piezoelectric plate is positively related to that of Rayleigh surface wave in a traction-free piezoelectric half-space. The edge wave velocity can be enhanced when the piezoelectric plate is considered as one with weaker anisotropy.

KEYWORDS

piezoelectric plate, edge wave, bending wave, dispersion relation, plate theory

Introduction

Edge waves, which propagate along the edge of a thin plate and decay transversely with distance from the edge, have attracted much attention in the past 60 years since the existence of a flexural wave guided by the free edge of a semi-infinite isotropic elastic thin plate was reported by Konenkov (1960). Edge waves have great potential for the applications in the measurement of material properties and non-destructive

evaluation of thin elastic structures, such as aircraft wings, submarine hulls, rotor blades, and so on (Lawrie and Kaplunov, 2012). In view of these important application, the existence and propagation of edge waves in various elastic thin plates, such as transversely isotropic plates (Piliposian et al., 2010), orthotropic plates (Norris, 1994; Thompson et al., 2002), cubic symmetric materials (Belubekyan and Engibaryan, 1996), anisotropic materials (Fu, 2003), and laminated plates (Liu et al., 1991; Zakharov and Becker, 2003; Fu and Brookes, 2006; Lu et al., 2007), have been well studied. Lawrie and Kaplunov (2012) gave a periodic overview of edge waves and resonance on elastic structures before the 2010s. Most of the above results were derived using Kirchhoff plate theory. It was demonstrated that the edge waves in elastic thin plate were also theoretically predicted by Mindlin plate theory including shear deformation and rotatory inertia (Norris et al., 1998) and Ambartsumian refined plate theory considering high-order shear deformation (Piliposian and Ghazaryan, 2011). The former was proved to be in agreement with experimental and finite element results (Lagasse and Oliner, 1976; Norris et al., 1998). It was shown that the velocity of edge waves predicted by Kirchhoff plate theory, which is valid only for very low frequency, is much larger than the results of experiment and finite element.

Piezoelectric materials are widely used to develop electro-mechanical transducers for converting mechanical energy to electric energy or *vice versa*, and acoustic wave devices for frequency operation and sensing. The subject of elastic wave propagation in various piezoelectric materials and structures has received increasing attention from the mechanics community in the last few decades. Recent results mainly include surface waves in piezoelectric half-space (Collet and Destrade, 2004; Collet and Destrade, 2005), elastic half-space covered by piezoelectric layer (Nie et al., 2020a; Zhang et al., 2022) or the reverse configuration (Liu and He, 2010; Huang et al., 2014), interface waves in piezoelectric bi-material (Yang and Yang, 2009; Otero et al., 2012), guided waves in piezoelectric plate (Zhang et al., 2012; Nie et al., 2020b), and multilayered plate (Gao and Zhang, 2020; Xia et al., 2021), functionally graded piezoelectric material (Liu et al., 2021; Lakshman, 2022) and so on. So far, most of the available results on elastic wave in piezoelectric materials and structures are for the infinite media extended in one or two dimensions. It is known that the vibration energy carried by edge waves can be confined to the edge region of the plate and decays rapidly with distance from the edge which means that there will be very little motion away from the active edge. This property has unique advantage in fixing and support of acoustic wave device compared to that of bulk wave and surface wave, since devices can be mounted to supporting structures at the side very close to the active edge without affecting the device performance. From this, the edge waves have great promise for achieving the miniaturisation of acoustic wave devices which is exactly demand for the future development of micro-electro-mechanical systems (MEMS). Compared with elastic waves

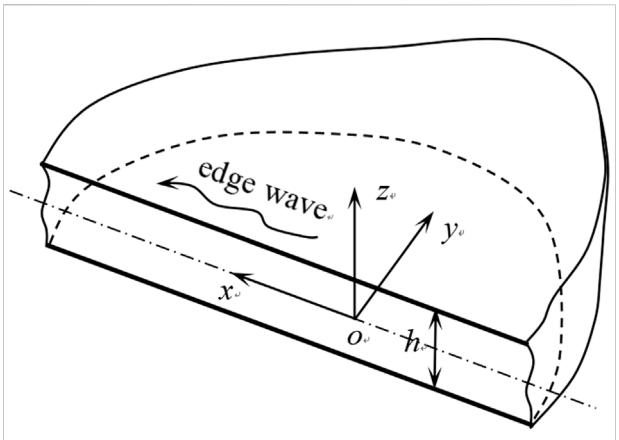

FIGURE 1
Geometry of a semi-infinite piezoelectric plate.

propagation in the infinite piezoelectric materials, which have been widely studied and also have been used in many engineering fields, the results related to edge waves in the thin piezoelectric plates are still limited, and some interesting properties are waiting to be further revealed. Recently, Piliposian and Ghazaryan (2011) studied the existence and propagation of bending waves localized at the free edge of a piezoelectric plate within the framework of Ambartsumian refined plate theory. The condition for existence of a localized bending wave was given. Nie et al. (2021) investigated bending waves propagation along the free edge of a semi-infinite piezoelectric plate perfectly bonded with a metal strip plate using the first-order Reissner-Mindlin refined plate theory. The propagation of bending wave with multi-mode was shown. Piezoelectric plates considered in (Piliposian and Ghazaryan, 2011) and (Nie et al., 2021) are both assumed as the transversely isotropic media. In this paper, we study the propagation of bending waves localized along the free edge of a semi-infinite piezoelectric plate of orthogonal symmetry using two-variable refined plate theory (TVPT, a high-order shear deformation theory), Reissner-Mindlin refined plate theory (RMPT, a first-order shear deformation theory), and the classical plate theory (CPT). Our aim is to examine the difference in dispersion property between the three plate theories and to reveal the effects of electrical boundary applied on the free edge and material property on wave propagation. To the best of our knowledge, the propagation of edge waves in an orthogonal piezoelectric plate has not been previously studied and also has not been analyzed in the context of TVPT.

Problem formulation and plate theories

A semi-infinite piezoelectric plate of thickness h is shown in Figure 1. The plate ($-\infty < x < \infty$; $0 \le y < \infty$; $-h/2 \le z \le h/2$) is

referred to rectangular coordinates (x, y, z) and is bounded by a free edge at $y = 0$. The plate is made of orthogonal piezoelectric medium with macroscopic symmetry of mm2 and is poled along z-direction. We consider bending wave propagating along the free edge of such plate. The constitutive relations of orthogonal piezoelectric medium are expressed as

$$\begin{bmatrix}\sigma_{xx}\\ \sigma_{yy}\\ \sigma_{zz}\\ \sigma_{yz}\\ \sigma_{xz}\\ \sigma_{xy}\end{bmatrix} = \begin{bmatrix} c_{11} & c_{12} & c_{13} & 0 & 0 & 0\\ & c_{22} & c_{23} & 0 & 0 & 0\\ & & c_{33} & 0 & 0 & 0\\ & & & c_{44} & 0 & 0\\ & \text{sym.} & & & c_{55} & 0\\ & & & & & c_{66}\end{bmatrix}\begin{bmatrix}\varepsilon_{xx}\\ \varepsilon_{yy}\\ \varepsilon_{zz}\\ \gamma_{yz}\\ \gamma_{xz}\\ \gamma_{xy}\end{bmatrix} - \begin{bmatrix} 0 & 0 & e_{31}\\ 0 & 0 & e_{32}\\ 0 & 0 & e_{33}\\ 0 & e_{24} & 0\\ e_{15} & 0 & 0\\ 0 & 0 & 0\end{bmatrix} \times \begin{bmatrix}E_x\\ E_y\\ E_z\end{bmatrix} \tag{1}$$

$$\begin{bmatrix}D_x\\ D_y\\ D_z\end{bmatrix} = \begin{bmatrix} 0 & 0 & 0 & 0 & e_{15} & 0\\ 0 & 0 & 0 & e_{24} & 0 & 0\\ e_{31} & e_{32} & e_{33} & 0 & 0 & 0\end{bmatrix}\begin{bmatrix}\varepsilon_{xx}\\ \varepsilon_{yy}\\ \varepsilon_{zz}\\ \gamma_{yz}\\ \gamma_{xz}\\ \gamma_{xy}\end{bmatrix} + \begin{bmatrix}\kappa_{11} & 0 & 0\\ 0 & \kappa_{22} & 0\\ 0 & 0 & \kappa_{33}\end{bmatrix}\begin{bmatrix}E_x\\ E_y\\ E_z\end{bmatrix} \tag{2}$$

where c_{ij}, κ_{ij} and e_{ij} ($i, j = 1$–6) are the elastic constants, dielectric and piezoelectric constants; σ_{kl}, ε_{kl}, E_k, and D_k (k, $l = x$, y, and z) are the stress, strain, electric field and electric displacement, respectively. The non-trivial strain-displacement and electric field-potential relations are as follows

$$\begin{aligned}&\varepsilon_{xx} = \frac{\partial u}{\partial x}, \varepsilon_{yy} = \frac{\partial v}{\partial y}, \gamma_{xy} = \frac{\partial u}{\partial y} + \frac{\partial v}{\partial x}\\ &\gamma_{yz} = \frac{\partial w}{\partial y} + \frac{\partial v}{\partial z}, \gamma_{xz} = \frac{\partial w}{\partial x} + \frac{\partial u}{\partial z},\\ &E_x = -\frac{\partial \varphi}{\partial x}, E_y = -\frac{\partial \varphi}{\partial y}, E_z = -\frac{\partial \varphi}{\partial z}.\end{aligned} \tag{3}$$

where u, v, and w are the mechanical displacement components along the x-axis, y-axis and z-axis; φ is the electric potential.

Two-variable refined plate theory

According to the TVPT (Shimpi, 2002; Shimpi and Patel, 2006), the transversal displacement w, which is independent of z, can be expressed as a combination of the bending component and the shear component, i.e.,

$$w(x, y, t) = w_b(x, y, t) + w_s(x, y, t) \tag{4}$$

where w_b and w_s denote the bending component and shear component of transversal displacement w, respectively.

Also, the in-plane displacements u and v consisting of bending and shear components are

$$u = u_b + u_s,\ v = v_b + v_s \tag{5}$$

where u_b and v_b represent the bending components of in-plane displacement u and v; u_s, and v_s are the shear components of u and v, respectively.

Assuming that the bending components of in-plane displacement u_b and v_b play the same roles as u and v in CPT, gives

$$u_b = -z\frac{\partial w_b}{\partial x},\ v_b = -z\frac{\partial w_b}{\partial y} \tag{6}$$

The shear components of in-plane displacement are considered as the following functions

$$u_s = f(z)\frac{\partial w_s}{\partial x},\ v_s = f(z)\frac{\partial w_s}{\partial y} \tag{7}$$

where $f(z)$ signifies the generalized shape function describing the transverse shear deformation and stress distribution through the thickness of the piezoelectric plate. In this two-variable refined plate theory (Shimpi, 2002; Shimpi and Patel, 2006), we assume.

$$f(z) = \frac{z}{4} - \frac{5z^3}{3h^2} \tag{8}$$

The mechanical displacements can be rewritten as

$$\begin{aligned}u(x, y, z, t) &= h\left[\frac{1}{4}\left(\frac{z}{h}\right) - \frac{5}{3}\left(\frac{z}{h}\right)^3\right]\frac{\partial w_s}{\partial x} - z\frac{\partial w_b}{\partial x}\\ v(x, y, z, t) &= h\left[\frac{1}{4}\left(\frac{z}{h}\right) - \frac{5}{3}\left(\frac{z}{h}\right)^3\right]\frac{\partial w_s}{\partial y} - z\frac{\partial w_b}{\partial y}\\ w(x, y, z, t) &= w_s(x, y, t) + w_b(x, y, t)\end{aligned} \tag{9}$$

The non-zero strains are

$$\begin{aligned}\varepsilon_{xx} &= -z\frac{\partial^2 w_b}{\partial x^2} + h\left[\frac{1}{4}\left(\frac{z}{h}\right) - \frac{5}{3}\left(\frac{z}{h}\right)^3\right]\frac{\partial^2 w_s}{\partial x^2},\\ \varepsilon_{yy} &= -z\frac{\partial^2 w_b}{\partial y^2} + h\left[\frac{1}{4}\left(\frac{z}{h}\right) - \frac{5}{3}\left(\frac{z}{h}\right)^3\right]\frac{\partial^2 w_s}{\partial y^2},\\ \gamma_{xy} &= -2z\frac{\partial^2 w_b}{\partial x \partial y} + 2h\left[\frac{1}{4}\left(\frac{z}{h}\right) - \frac{5}{3}\left(\frac{z}{h}\right)^3\right]\frac{\partial^2 w_s}{\partial x \partial y},\\ \gamma_{yz} &= \left[\frac{5}{4} - 5\left(\frac{z}{h}\right)^2\right]\frac{\partial w_s}{\partial y}, \gamma_{xz} = \left[\frac{5}{4} - 5\left(\frac{z}{h}\right)^2\right]\frac{\partial w_s}{\partial x}\end{aligned} \tag{10}$$

First-order Reissner-Mindlin refined plate theory

According to the RMPT (Reissner, 1945; Mindlin, 1951), the transversal displacement only includes a bending component and is also independent of z. The shear components of in-plane displacement vary linearly through the plate thickness. From this, the displacement fields for RMPT can be obtained by letting the shape function be linear, i.e., $f(z) = z$ in Eq. 9, which gives

$$u(x,y,z,t) = z\vartheta_x(x,y,t) - z\frac{\partial w}{\partial x}$$
$$v(x,y,z,t) = z\vartheta_y(x,y,t) - z\frac{\partial w}{\partial y} \tag{11}$$
$$w(x,y,z,t) = w(x,y,t)$$

where $w\ (x,y,t) = w_b\ (x,y,t)$ is the transversal displacement of middle plane of the plate. $\vartheta_x\ (x,y,t)$ and $\vartheta_y\ (x,y,t)$ are unknown functions defining transversal shears. The non-zero strains are reduced to

$$\varepsilon_{xx} = z\left(\frac{\partial\vartheta_x}{\partial x} - \frac{\partial^2 w}{\partial x^2}\right), \varepsilon_{yy} = z\left(\frac{\partial\vartheta_y}{\partial y} - \frac{\partial^2 w}{\partial y^2}\right),$$
$$\gamma_{xy} = z\left(\frac{\partial\vartheta_x}{\partial y} + \frac{\partial\vartheta_y}{\partial x} - 2\frac{\partial^2 w}{\partial x\partial y}\right), \gamma_{xz} = \vartheta_x, \gamma_{yz} = \vartheta_y \tag{12}$$

Classical plate theory

Neglect of the transversal shears, i.e., $\vartheta_x\ (x,y,t) = \vartheta_y\ (x,y,t) = 0$ in Eq. 12, we obtain displacement fields for the CPT

$$u(x,y,z,t) = -z\frac{\partial w}{\partial x}, v(x,y,z,t)$$
$$= -z\frac{\partial w}{\partial y}, w(x,y,z,t) \tag{13}$$
$$= w(x,y,t)$$

The non-zero strains can be further reduced to

$$\varepsilon_{xx} = -z\frac{\partial^2 w}{\partial x^2}, \varepsilon_{yy} = -z\frac{\partial^2 w}{\partial y^2}, \gamma_{xy} = -2z\frac{\partial^2 w}{\partial x\partial y} \tag{14}$$

For the above three plate theories, the distribution of the electric potential φ in the piezoelectric plate should satisfy the Maxwell equation which is approximately assumed as a combination of a half-cosine and linear variation (Quek and Wang, 2000; Ke et al., 2014)

$$\varphi = -\cos(\beta z)\phi(x,y,t) + \frac{2z\phi_0}{h} \tag{15}$$

where $\beta = \pi/h$. $\phi(x,y,t)$ is the spatial and time variation of the electric potential in the mid-plane of the piezoelectric plate. ϕ_0 is the value of the external electric voltage along z-direction.

Using Eq. 3, the electric fields can be written as

$$E_x = \cos(\beta z)\frac{\partial\phi}{\partial x}, E_y = \cos(\beta z)\frac{\partial\phi}{\partial y}, E_z = -\beta\sin(\beta z)\phi - \frac{2\phi_0}{h} \tag{16}$$

Derivation of governing equations

Two-variable refined plate theory

The strain energy Π_u of the piezoelectric plate is given by

$$\Pi_u = \frac{1}{2}\int_A\int_{-\frac{h}{2}}^{\frac{h}{2}}\left(\sigma_{xx}\varepsilon_{xx} + \sigma_{yy}\varepsilon_{yy} + \sigma_{yz}\gamma_{yz} + \sigma_{xz}\gamma_{xz} + \sigma_{xy}\gamma_{xy}\right)\mathrm{d}z\mathrm{d}A$$
$$-\frac{1}{2}\int_A\int_{-\frac{h}{2}}^{\frac{h}{2}}\left(-D_xE_x - D_yE_y - D_zE_z\right)\mathrm{d}z\mathrm{d}A \tag{17}$$

where A denotes the domain occupied by the mid-plane of piezoelectric plate. Substituting Eqs 10, 16 into Eq. 17 yields

$$\Pi_u = \frac{1}{2}\int_A\left(-M_{x1}\frac{\partial^2 w_b}{\partial x^2} + M_{x2}\frac{\partial^2 w_s}{\partial x^2} - M_{y1}\frac{\partial^2 w_b}{\partial y^2} + M_{y2}\frac{\partial^2 w_s}{\partial y^2}\right)\mathrm{d}A$$
$$+\frac{1}{2}\int_A\left(-M_{xy1}\frac{\partial^2 w_b}{\partial x\partial y} + M_{xy2}\frac{\partial^2 w_s}{\partial x\partial y} + Q_x\frac{\partial w_s}{\partial x} + Q_y\frac{\partial w_s}{\partial y}\right)\mathrm{d}A$$
$$-\frac{1}{2}\int_A\int_{-\frac{h}{2}}^{\frac{h}{2}}\left\{D_x\cos(\beta z)\frac{\partial\phi}{\partial x} + D_y\cos(\beta z)\frac{\partial\phi}{\partial y} - D_z\left[\beta\sin(\beta z)\phi + \frac{2\phi_0}{h}\right]\right\}\mathrm{d}z\mathrm{d}A \tag{18}$$

where the bending moments M_{x1}, M_{x2}, M_{y1} and M_{y2}, the twisting moments M_{xy1} and M_{xy2}, the shearing forces Q_x and Q_y, are respectively defined by

$$M_{x1} = \int_{-\frac{h}{2}}^{\frac{h}{2}}\sigma_{xx}z\mathrm{d}z = -\frac{h^3}{12}\left(c_{11}\frac{\partial^2 w_b}{\partial x^2} + c_{12}\frac{\partial^2 w_b}{\partial y^2}\right) + \frac{2he_{31}}{\pi}\phi \tag{19a}$$

$$M_{x2} = \int_{-\frac{h}{2}}^{\frac{h}{2}}\sigma_{xx}\left(\frac{z}{4} - \frac{5z^3}{3h^2}\right)\mathrm{d}z$$
$$= \frac{h^3}{1008}\left(c_{11}\frac{\partial^2 w_s}{\partial x^2} + c_{12}\frac{\partial^2 w_s}{\partial y^2}\right) - \frac{2he_{31}(\pi^2-10)}{\pi^3}\phi \tag{19b}$$

$$M_{y1} = \int_{-\frac{h}{2}}^{\frac{h}{2}}\sigma_{yy}z\mathrm{d}z = -\frac{h^3}{12}\left(c_{12}\frac{\partial^2 w_b}{\partial x^2} + c_{22}\frac{\partial^2 w_b}{\partial y^2}\right) + \frac{2he_{32}}{\pi}\phi \tag{19c}$$

$$M_{y2} = \int_{-\frac{h}{2}}^{\frac{h}{2}}\sigma_{yy}\left(\frac{z}{4} - \frac{5z^3}{3h^2}\right)\mathrm{d}z$$
$$= \frac{h^3}{1008}\left(c_{12}\frac{\partial^2 w_s}{\partial x^2} + c_{22}\frac{\partial^2 w_s}{\partial y^2}\right) - \frac{2he_{32}(\pi^2-10)}{\pi^3}\phi \tag{19d}$$

$$M_{xy1} = \int_{-\frac{h}{2}}^{\frac{h}{2}}2\sigma_{xy}z\mathrm{d}z = -\frac{h^3c_{66}}{3}\frac{\partial^2 w_b}{\partial x\partial y} \tag{19e}$$

$$M_{xy2} = \int_{-\frac{h}{2}}^{\frac{h}{2}}2\sigma_{xy}\left(\frac{z}{4} - \frac{5z^3}{3h^2}\right)\mathrm{d}z = \frac{h^3c_{66}}{252}\frac{\partial^2 w_s}{\partial x\partial y} \tag{19f}$$

$$Q_x = \int_{-\frac{h}{2}}^{\frac{h}{2}}\sigma_{xz}\left(\frac{5}{4} - \frac{5z^2}{h^2}\right)\mathrm{d}z = \frac{5hc_{55}}{6}\frac{\partial w_s}{\partial x} - \frac{20he_{15}}{\pi^3}\frac{\partial\phi}{\partial x} \tag{19g}$$

$$Q_y = \int_{-\frac{h}{2}}^{\frac{h}{2}}\sigma_{yz}\left(\frac{5}{4} - \frac{5z^2}{h^2}\right)\mathrm{d}z = \frac{5hc_{44}}{6}\frac{\partial w_s}{\partial y} - \frac{20he_{24}}{\pi^3}\frac{\partial\phi}{\partial y} \tag{19h}$$

The kinetic energy Π_k of the piezoelectric plate is calculated by

$$\begin{aligned}\Pi_k &= \frac{1}{2}\int_A \int_{-\frac{h}{2}}^{\frac{h}{2}} \rho\left[\left(\frac{\partial u}{\partial t}\right)^2 + \left(\frac{\partial v}{\partial t}\right)^2 + \left(\frac{\partial w}{\partial t}\right)^2\right] \mathrm{d}z\mathrm{d}A \\ &= \frac{\rho h^3}{24}\int_A \left\{\left[\frac{\partial}{\partial t}\left(\frac{\partial w_b}{\partial x}\right)\right]^2 + \left[\frac{\partial}{\partial t}\left(\frac{\partial w_b}{\partial y}\right)\right]^2\right\}\mathrm{d}A \\ &\quad + \frac{\rho h^3}{2016}\int_A \left\{\left[\frac{\partial}{\partial t}\left(\frac{\partial w_s}{\partial x}\right)\right]^2 + \left[\frac{\partial}{\partial t}\left(\frac{\partial w_s}{\partial y}\right)\right]^2\right\}\mathrm{d}A \\ &\quad + \frac{\rho h}{2}\int_A \left(\frac{\partial w_b}{\partial t} + \frac{\partial w_s}{\partial t}\right)^2 \mathrm{d}A \end{aligned} \tag{20}$$

The work done by external force Π_w is

$$\Pi_w = \frac{1}{2}\int_A \left[N_x\left(\frac{\partial w}{\partial x}\right)^2 + N_y\left(\frac{\partial w}{\partial y}\right)^2\right]\mathrm{d}A \tag{21}$$

where $N_x = -2e_{31}\phi_0$ and $N_y = -2e_{32}\phi_0$ are the normal forces induced by the external electric voltage ϕ_0 along the x- and y-axis, respectively.

The governing equations can be derived by Hamilton principle

$$\delta\int_0^t (\Pi_u - \Pi_w - \Pi_k)\mathrm{d}t = 0 \tag{22}$$

Substituting Eqs 18, 20, 21 into the above equation, letting the coefficients of δw_b, δw_s, and $\delta\phi$ be zero, the governing equations can be obtained as

$$\delta w_b\colon \frac{\partial^2 M_{x1}}{\partial x^2} + \frac{\partial^2 M_{y1}}{\partial y^2} + \frac{\partial^2 M_{xy1}}{\partial x\partial y} - N_x\left(\frac{\partial^2 w_b}{\partial x^2} + \frac{\partial^2 w_s}{\partial x^2}\right) - N_y\left(\frac{\partial^2 w_b}{\partial y^2} + \frac{\partial^2 w_s}{\partial y^2}\right) = \rho h\left(\frac{\partial^2 w_b}{\partial t^2} + \frac{\partial^2 w_s}{\partial t^2}\right) - \frac{\rho h^3}{12}\frac{\partial^2}{\partial t^2}\left(\frac{\partial^2 w_b}{\partial x^2} + \frac{\partial^2 w_b}{\partial y^2}\right) \tag{23a}$$

$$\delta w_s\colon \frac{\partial^2 M_{x2}}{\partial x^2} + \frac{\partial^2 M_{y2}}{\partial y^2} + \frac{\partial^2 M_{xy2}}{\partial x\partial y} - \frac{\partial Q_x}{\partial x} - \frac{\partial Q_y}{\partial y} - \frac{\rho h^3}{1008}\frac{\partial^2}{\partial t^2}\left(\frac{\partial^2 w_s}{\partial x^2} + \frac{\partial^2 w_s}{\partial y^2}\right) + \rho h\left(\frac{\partial^2 w_b}{\partial t^2} + \frac{\partial^2 w_s}{\partial t^2}\right) - N_x\left(\frac{\partial^2 w_b}{\partial x^2} + \frac{\partial^2 w_s}{\partial x^2}\right) - N_y\left(\frac{\partial^2 w_b}{\partial y^2} + \frac{\partial^2 w_s}{\partial y^2}\right) = 0 \tag{23b}$$

$$\delta\phi\colon \int_{-\frac{h}{2}}^{\frac{h}{2}}\left\{\frac{\partial D_x}{\partial x}\cos(\beta z) + \frac{\partial D_y}{\partial y}\cos(\beta z) + D_z[\beta\sin(\beta z)]\right\}\mathrm{d}z = 0 \tag{23c}$$

First-order Reissner-Mindlin refined plate theory

Using Hamilton principle and taking account of Eqs 12, 16, the governing equations for the RMPT can be obtained as

$$\delta\vartheta_x\colon \frac{\partial M_x}{\partial x} + \frac{\partial M_{xy}}{\partial y} - Q_x = \frac{\rho h^3}{12}\left(\frac{\partial^2\vartheta_x}{\partial t^2} - \frac{\partial^3 w}{\partial x\partial t^2}\right) \tag{24a}$$

$$\delta\vartheta_y\colon \frac{\partial M_y}{\partial y} + \frac{\partial M_{xy}}{\partial x} - Q_y = \frac{\rho h^3}{12}\left(\frac{\partial^2\vartheta_y}{\partial t^2} - \frac{\partial^3 w}{\partial y\partial t^2}\right) \tag{24b}$$

$$\delta w\colon \frac{\partial^2 M_x}{\partial x^2} + \frac{\partial^2 M_y}{\partial y^2} + \frac{\partial^2 M_{xy}}{\partial x\partial y} - N_x\frac{\partial^2 w}{\partial x^2} - N_y\frac{\partial^2 w}{\partial y^2} = \rho h\frac{\partial^2 w}{\partial t^2} + \frac{\rho h^3}{12}\frac{\partial^2}{\partial t^2}\left[\left(\frac{\partial\vartheta_x}{\partial x} + \frac{\partial\vartheta_y}{\partial y}\right) - \left(\frac{\partial^2 w}{\partial x^2} + \frac{\partial^2 w}{\partial y^2}\right)\right] \tag{24c}$$

$$\delta\phi\colon \int_{-\frac{h}{2}}^{\frac{h}{2}}\left\{\frac{\partial D_x}{\partial x}\cos(\beta z) + \frac{\partial D_y}{\partial y}\cos(\beta z) + D_z[\beta\sin(\beta z)]\right\}\mathrm{d}z = 0 \tag{24d}$$

where the bending moments M_x and M_y, the twisting moment M_{xy}, the shearing forces Q_x and Q_y, are respectively defined by

$$\begin{aligned} M_x &= \int_{-\frac{h}{2}}^{\frac{h}{2}} \sigma_{xx} z\mathrm{d}z \\ &= \frac{h^3}{12}\left[c_{11}\left(\frac{\partial\vartheta_x}{\partial x} - \frac{\partial^2 w}{\partial x^2}\right) + c_{12}\left(\frac{\partial\vartheta_y}{\partial y} - \frac{\partial^2 w}{\partial y^2}\right)\right] + \frac{2he_{31}}{\pi}\phi \end{aligned} \tag{25a}$$

$$\begin{aligned} M_y &= \int_{-\frac{h}{2}}^{\frac{h}{2}} \sigma_{yy} z\mathrm{d}z \\ &= \frac{h^3}{12}\left[c_{12}\left(\frac{\partial\vartheta_x}{\partial x} - \frac{\partial^2 w}{\partial x^2}\right) + c_{22}\left(\frac{\partial\vartheta_y}{\partial y} - \frac{\partial^2 w}{\partial y^2}\right)\right] + \frac{2he_{32}}{\pi}\phi \end{aligned} \tag{25b}$$

$$M_{xy} = \int_{-\frac{h}{2}}^{\frac{h}{2}} 2\sigma_{xy} z\mathrm{d}z = \frac{h^3 c_{66}}{6}\left(\frac{\partial\vartheta_x}{\partial y} + \frac{\partial\vartheta_y}{\partial x} - 2\frac{\partial^2 w}{\partial x\partial y}\right) \tag{25c}$$

$$Q_x = \int_{-\frac{h}{2}}^{\frac{h}{2}} \sigma_{xz}\mathrm{d}z = c_{55}h\vartheta_x - \frac{2he_{15}}{\pi}\frac{\partial\phi}{\partial x} \tag{25d}$$

$$Q_y = \int_{-\frac{h}{2}}^{\frac{h}{2}} \sigma_{yz}\mathrm{d}z = c_{44}h\vartheta_y - \frac{2he_{24}}{\pi}\frac{\partial\phi}{\partial y} \tag{25e}$$

Classical plate theory

The governing equations for CPT are

$$\begin{aligned}\delta w\colon \frac{\partial^2 M_x}{\partial x^2} + \frac{\partial^2 M_y}{\partial y^2} + \frac{\partial^2 M_{xy}}{\partial x\partial y} - N_x\frac{\partial^2 w}{\partial x^2} - N_y\frac{\partial^2 w}{\partial y^2} \\ = \rho h\frac{\partial^2 w}{\partial t^2} - \frac{\rho h^3}{12}\frac{\partial^2 w}{\partial t^2}\left(\frac{\partial^2 w}{\partial x^2} + \frac{\partial^2 w}{\partial y^2}\right)\end{aligned} \tag{26a}$$

$$\delta\phi\colon \int_{-\frac{h}{2}}^{\frac{h}{2}}\left\{\frac{\partial D_x}{\partial x}\cos(\beta z) + \frac{\partial D_y}{\partial y}\cos(\beta z) + D_z[\beta\sin(\beta z)]\right\}\mathrm{d}z = 0 \tag{26b}$$

where the bending moments M_x, M_y, and the twisting moment M_{xy} are

$$M_x = \int_{-\frac{h}{2}}^{\frac{h}{2}} \sigma_{xx} z\mathrm{d}z = -\frac{h^3}{12}\left(c_{11}\frac{\partial^2 w}{\partial x^2} + c_{12}\frac{\partial^2 w}{\partial y^2}\right) + \frac{2he_{31}}{\pi}\phi \tag{27a}$$

$$M_y = \int_{-\frac{h}{2}}^{\frac{h}{2}} \sigma_{yy} z \mathrm{d}z = -\frac{h^3}{12}\left(c_{12}\frac{\partial^2 w}{\partial x^2} + c_{22}\frac{\partial^2 w}{\partial y^2}\right) + \frac{2he_{32}}{\pi}\phi \quad (27b)$$

$$M_{xy} = \int_{-\frac{h}{2}}^{\frac{h}{2}} 2\sigma_{xy} z \mathrm{d}z = -\frac{h^3 c_{66}}{3}\frac{\partial^2 w}{\partial x \partial y} \quad (27c)$$

Solution of the localized bending waves

Two-variable refined plate theory

For bending wave propagating along x-direction we seek the general solution satisfying the governing Eq. 23 in the form

$$\begin{aligned} w_b(x,y,t) &= A\mathrm{e}^{bky}\mathrm{e}^{\mathrm{i}k(ct-x)}, \\ w_s(x,y,t) &= B\mathrm{e}^{bky}\mathrm{e}^{\mathrm{i}k(ct-x)}, \\ \phi(x,y,t) &= D\mathrm{e}^{bky}\mathrm{e}^{\mathrm{i}k(ct-x)} \end{aligned} \quad (28)$$

where $\mathrm{i} = \sqrt{-1}$, c is the phase velocity, k is the wavenumber, b is a parameter to be determined. A, B and D are unknown amplitudes. Substituting Eq. 28 into Eq. 23 and taking account of Eq. 19, we can obtain

$$\left\{\frac{\eta^2}{12}\left[c_{11} - 2(c_{12}+2c_{66})b^2 + c_{22}b^4 - \rho c^2(1-b^2)\right] + \frac{N_y}{h}b^2 - \frac{N_x}{h} - \rho c^2\right\}A + \left(\frac{N_y}{h}b^2 - \frac{N_x}{h} - \rho c^2\right)B + \frac{2}{\pi}(e_{31} - e_{32}b^2)D = 0 \quad (29a)$$

$$\left(\frac{N_y}{h}b^2 - \frac{N_x}{h} - \rho c^2\right)A + \left\{\begin{array}{l}\frac{\eta^2}{1008}\left[c_{11} - 2(c_{12}+2c_{66})b^2 + c_{22}b^4 - \rho c^2(1-b^2)\right] \\ +\frac{5}{6}(c_{55} - c_{44}b^2) + \frac{N_y}{h}b^2 - \frac{N_x}{h} - \rho c^2\end{array}\right\}B + \left[\frac{2(\pi^2-10)}{\pi^3}(e_{31} - e_{32}b^2) - \frac{20}{\pi^3}(e_{15} - e_{24}b^2)\right]D = 0 \quad (29b)$$

$$\frac{2}{\pi}(e_{31} - e_{32}b^2)A + \left[\frac{2(\pi^2-10)}{\pi^3}(e_{31} - e_{32}b^2) - \frac{20}{\pi^3}(e_{15} - e_{24}b^2)\right]B - \frac{1}{2}\left[(\kappa_{11} - \kappa_{22}b^2) + \frac{\pi^2}{\eta^2}\kappa_{33}\right]D = 0 \quad (29c)$$

where $\eta = kh$ is the non-dimensional wavenumber. Eq. 29 is a system of linear homogeneous equations with respect to the unknown amplitudes A, B and D. A non-trivial solution requires that the determinant of coefficient matrix of Eq. 29 vanishes which obtains a 10-order equation in undetermined parameter b. There are ten roots of b representing the propagation direction of the ten partial waves, respectively. In order to satisfy the attenuation condition that the displacements and electric potential should vanish as $y \to \infty$, we only take the five negative roots denoted by b_m (m = 1–5). The general solution to the governing equation can be rewritten as

$$\begin{aligned} w_b &= \sum_{m=1}^{5} A_m \mathrm{e}^{b_m ky}\mathrm{e}^{\mathrm{i}k(ct-x)}, \\ w_s &= \sum_{m=1}^{5} \alpha_m A_m \mathrm{e}^{b_m ky}\mathrm{e}^{\mathrm{i}k(ct-x)}, \\ \phi &= \sum_{m=1}^{5} \beta_m A_m \mathrm{e}^{b_m ky}\mathrm{e}^{\mathrm{i}k(ct-x)} \end{aligned} \quad (30)$$

where $\alpha_m = B_m/A_m$ and $\beta_m = D_m/A_m$ are amplitude ratios given in Appendix A.

At the free edge $y = 0$, the bending moments and twisting moments should be zero, i.e., $M_{y1} = M_{y2} = M_{xy1} = M_{xy2} = 0$. We further consider two types of electrical boundary conditions at the edge $y = 0$, i.e., $\int_{-h/2}^{h/2} D_y \mathrm{d}z = 0$ for electrically open case, and $\phi = 0$ for electrically shorted case. Substituting the general solution Eq. 30 into the above mechanical and electrical boundary conditions, a system of 5-order linear homogeneous equations with unknown amplitudes A_m yields, i.e., $\mathbf{T}\cdot\mathbf{A} = 0$, where $\mathbf{A} = [A_1, A_2, A_3, A_4, A_5]^{\mathrm{T}}$. Elements of matrix $\mathbf{T}$ for electrically open case at the free edge are given by

$$\begin{aligned} T_{1m} &= \frac{\eta^2}{12}(-c_{12} + c_{22}b_m^2) - \frac{2}{\pi}e_{32}\beta_m, \\ T_{2m} &= \frac{\eta^2}{1008}(-c_{12} + c_{22}b_m^2)\alpha_m - \frac{2(\pi^2-10)}{\pi^3}e_{32}\beta_m, \\ T_{3m} &= \frac{\eta^2}{3}c_{66}b_m,\ T_{4m} = \frac{\eta^2}{252}c_{66}b_m\alpha_m, \\ T_{5m} &= \frac{5\eta}{6}e_{24}b_m\alpha_m + \frac{2\eta}{\pi}\kappa_{22}b_m\beta_m \end{aligned} \quad (31)$$

The elements of matrix $\mathbf{T}$ for electrically shorted case are the same except for $T_{5m} = \beta_m$.

First-order Reissner-Mindlin refined plate theory

We consider the following solution satisfying the governing Eq. 24

$$\begin{aligned} \vartheta_x &= Aik\mathrm{e}^{bky}\mathrm{e}^{\mathrm{i}k(ct-x)}, \\ \vartheta_y &= Bk\mathrm{e}^{bky}\mathrm{e}^{\mathrm{i}k(ct-x)}, \\ w &= D\mathrm{e}^{bky}\mathrm{e}^{\mathrm{i}k(ct-x)}, \\ \phi &= F\mathrm{e}^{bky}\mathrm{e}^{\mathrm{i}k(ct-x)} \end{aligned} \quad (32)$$

where A, B, D and F are unknown amplitudes. Substituting Eq. 32 into Eq. 24 obtains

$$\frac{\eta^2}{12}\left(-c_{11} + c_{66}b^2 + \rho c^2 - \frac{12c_{55}}{\eta^2}\right)A - \frac{\eta^2 b}{12}(c_{12}+c_{66})B - \frac{\eta^2}{12}[c_{11} - (c_{12}+2c_{66})b^2 + \rho c^2]D - \frac{2}{\pi}(e_{31}+e_{15})F = 0 \quad (33a)$$

$$\frac{\eta^2 b}{12}(c_{12}+c_{66})A + \frac{\eta^2}{12}\left(b^2c_{22} - c_{66} + \rho c^2 - \frac{12c_{44}}{\eta^2}\right)B - \frac{\eta^2}{12}[b^3c_{22} - b(c_{12}+2c_{66}) - b\rho c^2]D + \frac{2b}{\pi}(e_{32}+e_{24})F = 0 \quad (33b)$$

$$\frac{\eta^2}{12}\left[-c_{11}+b^2(c_{12}+2c_{66})-\rho c^2\right]A+\frac{\eta^2}{12}\left[b^3c_{22}-b(c_{12}+2c_{66})-b\rho c^2\right]B$$
$$-\frac{\eta^2}{12}\left[c_{11}-2b^2(c_{12}+2c_{66})+b^4c_{22}-\frac{12}{\eta^2}\rho c^2-\frac{12}{\eta^2 h}\left(N_x-b^2N_y\right)-\rho c^2\left(1-b^2\right)\right]D$$
$$-\frac{2}{\pi}(e_{31}-b^2e_{32})F=0 \tag{33c}$$

$$\frac{2}{\pi}(e_{15}+e_{31})A+\frac{2b}{\pi}(e_{24}+e_{32})B+\frac{2}{\pi}(e_{31}-b^2e_{32})D$$
$$-\frac{1}{2}\left(\kappa_{11}-b^2\kappa_{22}+\frac{\pi^2\kappa_{33}}{\eta^2}\right)F=0 \tag{33d}$$

Equation 33 is a system of linear homogeneous equations with respect to the unknown amplitudes A, B, D, and F. A non-trivial solution requires that the determinant of coefficient matrix vanishes which obtains an 8-order equation in b. To satisfy the attenuation condition, only the four negative roots denoted by b_n (n = 1–4) are remained. The general solution can be written as

$$\vartheta_x=\sum_{n=1}^{4}A_n ike^{b_nky}e^{ik(ct-x)},\ \vartheta_y=\sum_{n=1}^{4}\alpha_nA_nke^{b_nky}e^{ik(ct-x)},$$
$$w=\sum_{n=1}^{4}\beta_nA_ne^{b_nky}e^{ik(ct-x)},\ \phi=\sum_{n=1}^{4}\chi_nA_ne^{b_nky}e^{ik(ct-x)} \tag{34}$$

where $\alpha_n = B_n/A_n$, $\beta_n = D_n/A_n$, and $\chi_n = F_n/A_n$ are amplitude ratios given in Appendix B.

At the free edge $y = 0$, the bending moment, twisting moment and shear force should be zero, i.e., $M_y = M_{xy} = Q_y = 0$. The electrical boundary conditions at the free edge are the same as the case of TVPT. Using the general solution Eq. 34 and the corresponding boundary conditions, a system of 4-order linear homogeneous equations with unknown amplitudes A_n can be obtained, i.e., $\mathbf{T}\cdot\mathbf{A}=0$, where $\mathbf{A}=[A_1, A_2, A_3, A_4]^{\mathrm{T}}$. Elements of matrix $\mathbf{T}$ for electrically open case are

$$T_{1n}=\frac{\eta^2h}{12}\left[c_{12}(1+\beta_n)+c_{22}(b_n\alpha_n-b_n^2\beta_n)\right]+\frac{2he_{32}}{\pi}\chi_n,$$
$$T_{2n}=\frac{i\eta^2hc_{66}}{12}(b_n-\alpha_n+2b_n\beta_n),T_{3n}=\eta\left(c_{44}\alpha_n-\frac{2b_ne_{24}}{\pi}\chi_n\right),$$
$$T_{4n}=\frac{2\eta e_{24}}{\pi}\alpha_n+\frac{\eta b_n\kappa_{22}}{2}\chi_n \tag{35}$$

The elements of matrix $\mathbf{T}$ for electrically shorted case are the same except for $T_{4n} = \chi_n$.

Classical plate theory

We consider the following solution of Eq. 26

$$w=Ke^{bky}e^{ik(ct-x)},\ \phi=Je^{bky}e^{ik(ct-x)} \tag{36}$$

where K and J are unknown amplitudes. Substituting Eq. 36 into Eq. 26 obtains

$$\left\{\frac{\eta^2}{12}\left[c_{11}-2(c_{12}+2c_{66})b^2+c_{22}b^4-\rho c^2\left(1-b^2\right)\right]+\frac{N_y}{h}b^2\right.$$
$$\left.-\frac{N_x}{h}-\rho c^2\right\}K+\frac{2}{\pi}(e_{31}-e_{32}b^2)J=0 \tag{37a}$$

$$\frac{2}{\pi}(e_{31}-e_{32}b^2)K+\left[\frac{1}{2}\left(-\kappa_{11}+\kappa_{22}b^2\right)-\frac{\pi^2}{2\eta^2}\kappa_{33}\right]J=0 \tag{37b}$$

Equation 37 is a system of linear homogeneous equations with respect to the unknown amplitudes K and J. A non-trivial solution requires that the determinant of coefficient matrix vanishes which yields a 6-order equation in b. To satisfy the attenuation condition, we only take the three negative roots denoted by b_j (j = 1–3). Eq. 36 is rewritten as

$$w=\sum_{j=1}^{3}K_je^{b_jky}e^{ik(ct-x)},\ \phi=\sum_{j=1}^{3}\beta_jK_je^{b_jky}e^{ik(ct-x)} \tag{38}$$

where β_j is the amplitude ratio given by

$$\beta_j=\frac{4\eta^2\left(e_{31}-e_{32}b_j^2\right)}{\eta^2\pi\left(\kappa_{11}-\kappa_{22}b_j^2\right)+\pi^3\kappa_{33}} \tag{39}$$

At the edge $y = 0$, the traction-free criterion requires $M_y = M_{xy} = 0$. Based on the general solution Eq. 38 and the corresponding boundary conditions, a system of 3-order linear homogeneous equations with constants A_j can be obtained, i.e., $\mathbf{T}\cdot\mathbf{A}=0$, where $\mathbf{A}=[A_1, A_2, A_3]^{\mathrm{T}}$. Elements of matrix $\mathbf{T}$ for electrically open condition are

$$T_{1j}=-\frac{h\eta^2}{12}\left(c_{12}-c_{22}b_j^2\right)-\frac{2h}{\pi}e_{32}\beta_j,\ T_{2j}=\frac{h\eta^2}{3}c_{66}b_j,\ T_{3j}=\frac{2\eta}{\pi}\kappa_{22}b_j\beta_j \tag{40}$$

The elements of matrix $\mathbf{T}$ for electrically shorted case are the same except for $T_{3j} = \beta_j$.

When the determinant of the matrix $\mathbf{T}$ carried out within the framework of TVPT, RMPT and CPT vanishes, we obtain the dispersion relations for localized bending waves propagating in the semi-infinite piezoelectric plate.

Numerical results and discussions

In this section, we give some numerical results to demonstrate the dispersion property of localized bending waves propagating along the free edge of an orthogonal piezoelectric plate. The piezoelectric plate is considered as PZN-0.07PT with material constants listed in Table 1 (Zhang et al., 2002).

Based on the dispersion relations derived using TVPT, RMPT and CPT, we calculate the dispersion curves of localized bending waves for the three plate theories shown in Figure 2, where boundary condition at the free edge is imposed as electrically open case, the external electric voltage $\phi_0 = 0$. It is noted that the difference between these three plate theories mainly lies in the

TABLE 1 Material constants used in the numerical examples.

Materials	c_{ij} (10^{10} Nm^{-2})									ρ (kg m^{-3})	e_{ij} (C m^{-2})					κ_{ij}/κ_0		
	c_{11}	c_{12}	c_{13}	c_{22}	c_{23}	c_{33}	c_{44}	c_{55}	c_{66}	ρ	e_{31}	e_{32}	e_{33}	e_{15}	e_{24}	κ_{11}/κ_0	κ_{22}/κ_0	κ_{33}/κ_0
PZN-0.07PT	14.5	15.3	12.7	18.0	15.0	14.1	6.5	0.34	7.1	8,038	−8.65	−17.44	3.69	6.25	3.24	6,953	1847	291
PZN-0.09PT	9.7	10.2	9.6	12.4	11.9	12.8	6.6	0.33	6.1	8,316	−7.85	−16.35	2.35	6.72	7.85	800	1,133	678
PIN-0.47PMN-0.28PT	18.3	9.8	3.6	11.9	11.5	18.0	6.4	0.67	5.0	8,125	−6.5	−18.65	6.48	17.78	12.91	6,164	2059	3,503

Where $\kappa_0 = 8.854 \times 10^{-12}$ F m^{-1} is the dielectric constant of vacuum.

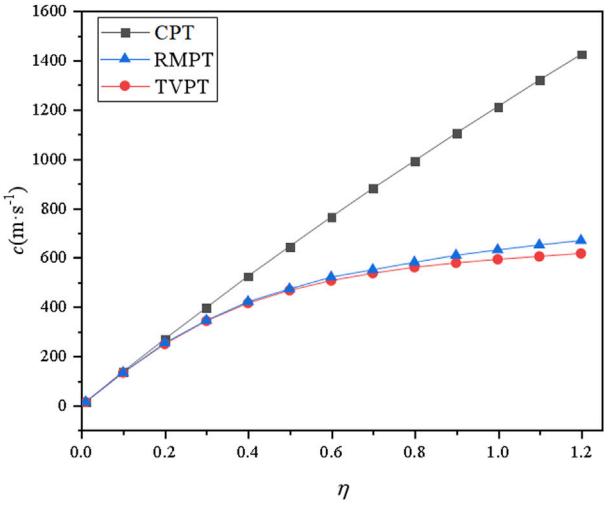

FIGURE 2
Dispersion curves of localized bending waves for different plate theories.

TABLE 2 Phase velocity of different electrical conditions at the free edge calculated by TVPT.

η	Phase velocity of electrically open case (m s^{-1})	Phase velocity of electrically shorted case (m s^{-1})
0.01	12.9998	12.9998
0.05	67.99983	67.99982
0.10	131.9997	131.9996
0.15	191.9995	191.9994
0.20	247.9994	247.9992
0.25	297.9993	297.9990
0.30	341.9992	341.9989
0.35	379.9991	379.9990
0.40	413.9989	413.9988
0.45	441.9989	441.9986
0.50	465.9989	465.9986

shape function $f(z)$ defining the transverse shear deformation along the thickness of the piezoelectric plate. $f(z)$ is shown as a cubic order in the z-thickness direction for TVPT, a linear function for RMPT, and zero for CPT, respectively. It is found from Figure 2 that the bending wave velocity for CPT is the highest, followed by RMPT, and TVPT is the lowest. The dispersion curves predicted by TVPT and RMPT are very close over the complete frequency range, while there is a significant difference in wave velocity between CPT result and the two results above, especially for high non-dimensional wavenumber η. The acceptable difference for the three plate theories is only within the range of very low non-dimensional wavenumber η (less than 0.2). It is known that edge wave velocity predicted by the first-order Mindlin plate theory agrees with experimental and finite element results (Lagasse and Oliner, 1976; Norris et al., 1998). Our calculation shows a very small difference between TVPT and RMPT which verifies the validity of the present results. Generally, the classical plate theory, which commonly neglects the effect of transverse shear and results in the overestimated wave velocity, is valid only for very low wavenumber and thin plate. The high-order plate theories are more accurate than first-order plate theories and are more applicable to the applications of high frequencies and thick plates. These results show that both TVPT and RMPT are valid for the analysis of edge waves in a piezoelectric plate and, to a certain extent, TVPT is more accurate than RMPT for high wavenumber and thick plate where CPT is not valid.

Based on the dispersion relations derived by TVPT, we calculate the phase velocity and group velocity of localized bending waves for electrically open case and shorted case listed in Tables 2, 3, respectively. The group velocity c_g is calculated through $c_g = c + kdc/dk$. It is observed that the phase velocity and group velocity of electrically open case are slightly larger than that of electrically shorted case. In view of the unnoticeable differences in phase velocity and group velocity between the two electrical boundary conditions, one can ignore the effect of electrical boundary imposed at the free edge when propagation of localized edge waves in a piezoelectric plate is considered. The

TABLE 3 Group velocity of different electrical conditions at the free edge calculated by TVPT.

η	Group velocity of electrically open case (m s^{-1})	Group velocity of electrically shorted case (m s^{-1})
0.01	26.62703	26.62702
0.05	134.1109	134.1102
0.10	255.9993	255.9992
0.15	365.9991	365.9988
0.20	459.9989	459.9984
0.25	532.9988	532.9983
0.30	587.9987	587.9985
0.35	631.9982	631.9980
0.40	675.9991	675.9977
0.45	695.9981	695.9980
0.50	707.9979	707.9978

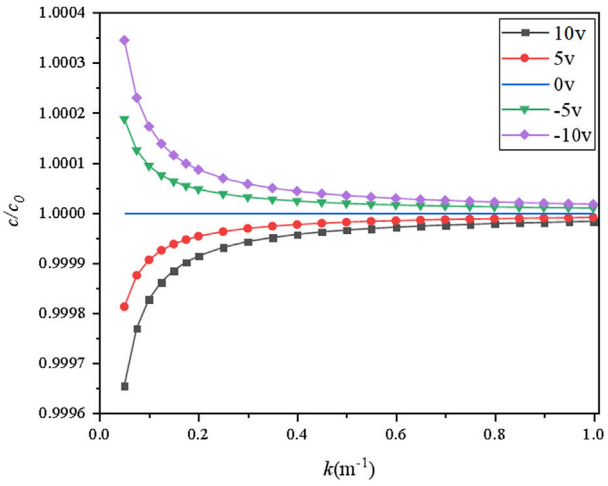

FIGURE 3
Effect of external electric voltage on phase velocity of localized bending waves.

acceptable results can be obtained through either electrically open boundary condition or electrically shorted boundary condition.

Figure 3 shows the effect of external electric voltage ϕ_0 on phase velocity of localized bending waves, where c_0 is the phase velocity for the case of $\phi_0 = 0$, the plate thickness $h = 1$ mm. It is found that the external electric voltage affects the phase velocity in the range of low wavenumber. There is nearly no effect when wavenumber is high enough. The wave velocity can be enlarged when a negative electric voltage is applied. On the contrary, wave velocity decreases under the influence of a positive electric voltage. For a given wavenumber, the wave velocity becomes larger as the magnitude of electric voltage becomes larger.

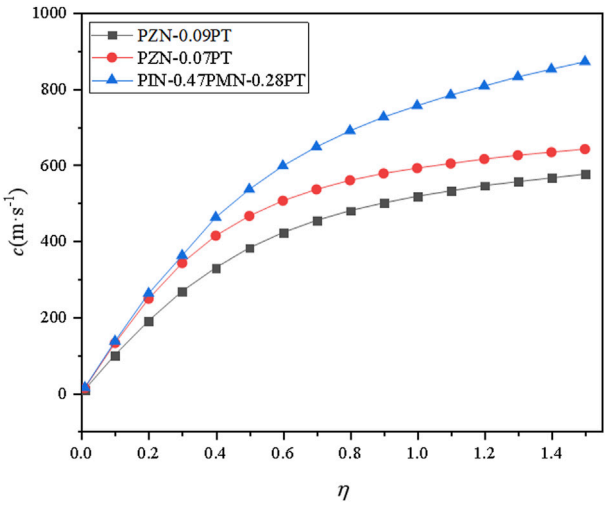

FIGURE 4
Dispersion curves for different piezoelectric materials.

To demonstrate the effect of material property on dispersion curve of localized bending waves we calculate the wave velocities for three different piezoelectric materials all with symmetry of orthogonal *mm*2, i.e., PZN-0.07PT, PZN-0.09PT and PIN-0.47PMN-0.28PT. The used material constants are found in Table 1 (Zhang et al., 2002; He et al., 2011; Zhang et al., 2011). Figure 4 shows the dispersion curves of the above three piezoelectric plates for electrically shorted case at the free edge, where $\phi_0 = 0$. It is known that the propagation of edge waves in a semi-infinite isotropic elastic plate is the analogue of the classical Rayleigh surface wave in a traction-free half-space under plane strain. We thus calculate the Rayleigh surface wave velocities of the considered three piezoelectric materials for the corresponding electrical boundary condition using plane strain model which are given by 1,599.9, 1,127.5, and 1902.3 ms^{-1} for PZN-0.07PT, PZN-0.09PT, and PIN-0.47PMN-0.28PT, respectively. Combined Figure 4 and Rayleigh surface wave velocities calculated, it is observed that the velocity of bending edge waves is positively related to that of Rayleigh surface wave, the larger the Rayleigh surface wave velocity the faster the localized bending wave propagation along the edge of the semi-infinite piezoelectric plate.

To reveal the effect of anisotropy on dispersion property of bending edge waves, comparison of dispersion characteristics for orthogonal piezoelectric plate (class mm2) and for transverse isotropic piezoelectric plate (class 6 mm) in the context of TVPT, is shown in Figure 5. The materials parameters used in this calculation are taken as follows: PZN-0.07PT is used as the mm2 piezoelectric plate whose material constants is found in Table 1; the 6 mm piezoelectric plate is reduced by assuming $c_{22} = c_{11} = 18\ \mathrm{Nm}^{-2} \times 10^{10}\ \mathrm{Nm}^{-2}$, $c_{23} = c_{13} = 15\ \mathrm{Nm}^{-2} \times 10^{10}\ \mathrm{Nm}^{-2}$, $c_{55} = c_{44} = 0.34\ \mathrm{Nm}^{-2} \times 10^{10}\ \mathrm{Nm}^{-2}$, $e_{24} = e_{15} = 3.24\ \mathrm{cm}^{-2}$, $e_{32} = e_{31} = -17.44\ \mathrm{cm}^{-2}$, and $\kappa_{22} = \kappa_{11} = 1847\kappa_0$ from the PZN-0.07PT. It is

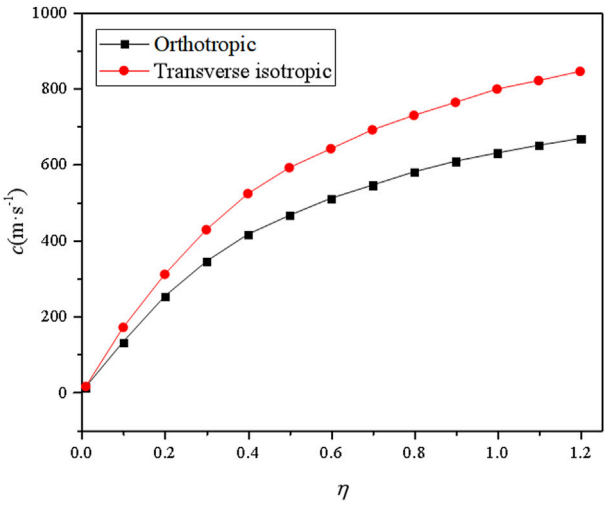

FIGURE 5
Comparison of the dispersion characteristics of bending edge waves in mm^2 piezoelectric plate and 6 mm piezoelectric plate under TVPT.

shown from Figure 5 that the edge wave velocity of the 6 mm piezoelectric plate is higher than the mm2 piezoelectric plate, for a fixed non-dimensional wavenumber η. It means that the wave velocity of bending edge wave increases when the piezoelectric plate is considered as a weaker anisotropic medium.

Conclusion

Propagation of localized bending waves along the free edge of a semi-infinite piezoelectric plate of orthogonal mm2 is studied using TVPT, RMPT, and CPT. The dispersion relations for electrically open and shorted cases at the free edge are obtained analytically. The difference in wave velocity between the three plate theories is analyzed. The effects of electrical boundary condition at the edge, material property as well as the external electric voltage on dispersion characteristic are discussed through some numerical examples. It is found that the wave velocity calculated by TVPT and RMPT are very close over the complete frequency range, which means both the two theories are valid for the analysis of edge waves in a piezoelectric plate. But CPT result, which shows a significant difference in wave velocity comparing with that of TVPT and RMPT, is unacceptable for high frequency and thick plate. The electrically boundary condition at the free edge of the semi-infinite piezoelectric plate has an insignificant effect on phase velocity and group velocity. Either electrically open boundary or electrically shorted boundary can produce an acceptable result. The velocity of bending edge waves in a piezoelectric plate is positively related to that of Rayleigh surface wave in a traction-free piezoelectric half-space. A large velocity of Rayleigh surface wave results in a large velocity of bending wave propagating along the edge of a semi-infinite piezoelectric plate. The edge wave velocity is enhanced when the piezoelectric plate is considered as a weaker anisotropic medium.

Data availability statement

The original contributions presented in the study are included in the article/Supplementary Material, further inquiries can be directed to the corresponding author.

Author contributions

GN: Conceptualization, methodology, formal analysis, writing-original draft. ZL: software, visualization. JL: conceptualization, writing-review and editing. LZ: methodology, writing-review and editing.

Funding

This study is supported by the National Natural Science Foundation of China (Nos. 11872041 and 11802185), the Natural Science Foundation of Hebei Province of China (No. A2019210203) and the Top-notch Young Talent Program of Hebei Province Education Department of China (No. BJK2022055).

Conflict of interest

The authors declare that the research was conducted in the absence of any commercial or financial relationships that could be construed as a potential conflict of interest.

Publisher's note

References

Belubekyan, M. V., and Engibaryan, A. I. (1996). Waves localized along the free edge of a plate with cubic symmetry. *Mech. Solids [MTT]* 31 (6), 117.

Collet, B., and Destrade, M. (2005). Explicit secular equations for piezoacoustic surface waves: Rayleigh modes. *J. Appl. Phys.* 98, 054903. doi:10.1063/1.2031948

Collet, B., and Destrade, M. (2004). Explicit secular equations for piezoacoustic surface waves: Shear-horizontal modes. *J. Acoust. Soc. Am.* 116 (6), 3432–3442. doi:10.1121/1.1819503

Fu, Y. B., and Brookes, D. W. (2006). Edge waves in asymmetrically laminated plates. *J. Mech. Phys. Solids* 54 (1), 1–21. doi:10.1016/j.jmps.2005.08.007

Fu, Y. B. (2003). Existence and uniqueness of edge waves in a generally anisotropic elastic plate. *Q. J. Mech. Appl. Math.* 56 (4), 605–616. doi:10.1093/qjmam/56.4.605

Gao, Q., and Zhang, Y. H. (2020). An accurate method for guided wave propagation in multilayered anisotropic piezoelectric structures. *Acta Mech.* 231, 1783–1804. doi:10.1007/s00707-020-02619-5

He, C. J., Jing, W. P., and Wang, F. F. (2011). Full tensorial elastic, piezoelectric, and dielectric properties characterization of [011]-poled PZN-9%PT single crystal. *IEEE Trans. Ultrason. Ferroelectr. Freq. Control* 58 (6), 1127–1130. doi:10.1109/tuffc.2011.1921

Huang, N. X., Lu, T. Q., Zhang, R., Wang, Y. L., and Cao, W. W. (2014). Guided wave propagation in a gold electrode film on a $Pb(Mg_{1/3}Nb_{2/3})O_{3\text{-}33\%}PbTiO_3$ ferroelectric single crystal substrate. *Chin. Phys. Lett.* 31 (10), 104302. doi:10.1088/0256-307x/31/10/104302

Ke, L. L., Wang, Y. S., Yang, J., and Kitipornchai, S. (2014). Free vibration of size-dependent magneto-electro-elastic nanoplates based on the nonlocal theory. *Acta Mech. Sin.* 30, 516–525. doi:10.1007/s10409-014-0072-3

Konenkov, Y. K. (1960). A Rayleigh-type flexural wave. *Sov. Phys. Acoust.* 6 (1), 122

Lagasse, P. E., and Oliner, A. A. (1976). Acoustic flexural mode on a ridge of semi-infinite height. *Electron. Lett.* 12 (1), 11–13. doi:10.1049/el:19760009

Lakshman, A. (2022). Propagation characteristic of Love-type wave in different types of functionally graded piezoelectric layered structure. *Waves Random Complex Media* 32 (3), 1424–1446. doi:10.1080/17455030.2020.1822562

Lawrie, J. B., and Kaplunov, J. (2012). Edge waves and resonance on elastic structures: An overview. *Math. Mech. Solids* 17 (1), 4–16. doi:10.1177/1081286511412281

Liu, C. C., Yu, J. G., Zhang, B., Zhang, X., and Elmaimouni, L. (2021). Analysis of Lamb wave propagation in a functionally graded piezoelectric small-scale plate based on the modified couple stress theory. *Compos. Struct.* 265, 113733. doi:10.1016/j.compstruct.2021.113733

Liu, G. R., Tani, J., Ohyoshi, T., and Watanabe, K. (1991). Characteristics of surface wave propagation along the edge of an anisotropic laminated semi-infinite plate. *Wave Motion* 13 (3), 243–251. doi:10.1016/0165-2125(91)90061-r

Liu, J. S., and He, S. T. (2010). Properties of Love waves in layered piezoelectric structures. *Int. J. Solids Struct.* 47 (2), 169–174. doi:10.1016/j.ijsolstr.2009.06.018

Lu, P., Chen, H. B., Lee, H. P., and Lu, C. (2007). Further studies on edge waves in anisotropic elastic plates. *Int. J. Solids Struct.* 44 (7-8), 2192–2208. doi:10.1016/j.ijsolstr.2006.07.005

Mindlin, R. D. (1951). Influence of rotatory inertia and shear on flexural motions of isotropic, elastic plates. *J. Appl. Mech.* 18, 31–38. doi:10.1115/1.4010217

Nie, G. Q., Dai, B., Liu, J. X., and Zhang, L. (2021). Bending waves in a semi-infinite piezoelectric plate with edge coated by a metal strip plate. *Wave Motion* 103 (4), 102731. doi:10.1016/j.wavemoti.2021.102731

Nie, G. Q., Zhang, K. K., and Liu, J. X. (2020). Love-type wave in PMN-PT single crystal layered structures with periodic undulations. *Int. J. Acoust. Vib.* 25 (2), 173–182. doi:10.20855/ijav.2020.25.21544

Nie, G. Q., Zhang, K. K., Liu, J. X., and Zhang, L. (2020). Effect of periodic corrugation on Lamb wave propagation in PMN-PT single crystal bilayer plates. *Ultrasonics* 108, 106176. doi:10.1016/j.ultras.2020.106176

Norris, A. N. (1994). Flexural edge waves. *J. Sound Vib.* 171 (4), 571–573. doi:10.1006/jsvi.1994.1141

Norris, A. N., Krylov, V. V., and Abrahams, I. D. (1998). Flexural edge waves and Comments on "A new bending wave solution for the classical plate equation" [J. Acoust. Soc. Am.**104**, 2220–2222 (1998)]. *J. Acoust. Soc. Am.The J. Acoust. Soc. Am.* 104107 (3), 22201781–22221784. doi:10.1121/1.428457

Otero, J. A., Ramos, R. R., Castillero, J. B., and Monsivais, G. (2012). Interfacial waves between two piezoelectric half-spaces with electro-mechanical imperfect interface. *Philos. Mag. Lett.* 92 (10), 534–540. doi:10.1080/09500839.2012.698758

Piliposian, G. T., Belubekyan, M. V., and Ghazaryan, K. B. (2010). Localized bending waves in a transversely isotropic plate. *J. Sound Vib.* 329 (17), 3596–3605. doi:10.1016/j.jsv.2010.03.019

Piliposian, G. T., and Ghazaryan, K. B. (2011). Localized bending vibrations of piezoelectric plates. *Waves Random Complex Media* 23 (3), 418–433. doi:10.1080/17455030.2011.576712

Quek, S. T., and Wang, Q. (2000). On dispersion relations in piezoelectric coupled-plate structures. *Smart Mat. Struct.* 9 (6), 859–867. doi:10.1088/0964-1726/9/6/317

Reissner, E. (1945). The effect of transverse shear deformation on the bending of elastic plates. *J. Appl. Mech.* 12 (3), 69–77. doi:10.1115/1.4009435

Shimpi, R. P., and Patel, H. G. (2006). A two variable refined plate theory for orthotropic plate analysis. *Int. J. Solids Struct.* 43 (22-23), 6783–6799. doi:10.1016/j.ijsolstr.2006.02.007

Shimpi, R. P. (2002). Refined plate theory and its variants. *AIAA J.* 40 (1), 137–146. doi:10.2514/3.15006

Thompson, I., Abrahams, I. D., and Norris, A. N. (2002). On the existence of flexural edge waves on thin orthotropic plates. *J. Acoust. Soc. Am.* 112 (5), 1756–1765. doi:10.1121/1.1506686

Xia, R. Y., Zhu, J. Y., Yi, J. L., Shao, S., and Li, Z. (2021). Guided wave propagation in multilayered periodic piezoelectric plate with a mirror plane. *Int. J. Mech. Sci.* 204 (2), 106539. doi:10.1016/j.ijmecsci.2021.106539

Yang, Z. T., and Yang, J. S. (2009). Effects of electric field gradient on the propagation of short piezoelectric interface waves. *Int. J. Appl. Electromagn. Mech.* 29 (2), 101–108. doi:10.3233/jae-2009-1006

Zakharov, D. D., and Becker, W. (2003). Rayleigh type bending waves in anisotropic media. *J. Sound Vib.* 261 (5), 805–818. doi:10.1016/s0022-460x(02)00996-3

Zhang, C. L., Chen, W. Q., and Zhang, C. Z. (2012). On propagation of anti-plane shear waves in piezoelectric plates with surface effect. *Phys. Lett. A* 376 (45), 3281–3286. doi:10.1016/j.physleta.2012.09.027

Zhang, L. L., Zhao, J., Nie, G. Q., and Liu, J. (2022). Propagation of Rayleigh-type surface waves in a layered piezoelectric nanostructure with surface effects. *Appl. Math. Mech.* 43 (3), 327–340. doi:10.1007/s10483-022-2824-7

Zhang, R., Jiang, B., Cao, W. W., and Amin, A. (2002). Complete set of material constants of $0.93Pb(Zn_{1/3}Nb_{2/3})O_3\text{-}0.07PbTiO_3$ domain engineered single crystal. *J. Mater. Sci. Lett.* 21 (23), 1877–1879. doi:10.1023/a:1021573431692

Zhang, Y. Y., Liu, D. A., Zhang, Q. H., Wang, W., Ren, B., Zhao, X., et al. (2011). Complete set of material constants of 011-poled rhombohedral single-crystal $0.25Pb(In_{1/2}Nb_{1/2})O_3\text{-}\ 0.47Pb(Mg_{1/3}Nb_{2/3})O_{3\text{-}0.28}PbTiO_3$. *J. Electron. Mat.* 40 (1), 92–96. doi:10.1007/s11664-010-1390-2

Appendix A

The expressions of A_m, B_m and D_m related to the amplitude ratios α_m and β_m are given by

$$A_m = \begin{vmatrix} \frac{\eta^2}{1008}\left[c_{11} - 2\left(c_{12} + 2c_{66}\right)b_m^2 + c_{22}b_m^4 - \rho c^2\left(1 - b_m^2\right)\right] & \frac{2\left(\pi^2 - 10\right)}{\pi^3}\left(e_{31} - e_{32}b_m^2\right) - \frac{20}{\pi^3}\left(e_{15} - e_{24}b_m^2\right) \\ +\frac{5}{6}\left(c_{55} - c_{44}b_m^2\right) + \frac{N_y}{h}b_m^2 - \frac{N_x}{h} - \rho c^2 & \\ -\frac{20}{\pi^3}\left(e_{15} - e_{24}b_m^2\right) + \frac{2\left(\pi^2 - 10\right)}{\pi^3}\left(e_{31} - e_{32}b_m^2\right) & -\frac{1}{2}\left(\kappa_{11} - \kappa_{22}b_m^2\right) - \frac{\pi^2}{2\eta^2}\kappa_{33} \end{vmatrix}$$

$$B_m = \begin{vmatrix} -\frac{N_y}{h}b_m^2 + \frac{N_x}{h} + \rho c^2 & \frac{2\left(\pi^2 - 10\right)}{\pi^3}\left(e_{31} - e_{32}b_m^2\right) - \frac{20}{\pi^3}\left(e_{15} - e_{24}b_m^2\right) \\ -\frac{2}{\pi}\left(e_{31} - e_{32}b_m^2\right) & -\frac{1}{2}\left(\kappa_{11} - \kappa_{22}b_m^2\right) - \frac{\pi^2}{2\eta^2}\kappa_{33} \end{vmatrix}$$

$$D_m = \begin{vmatrix} \frac{\eta^2}{1008}\left[c_{11} - 2\left(c_{12} + 2c_{66}\right)b_m^2 + c_{22}b_m^4 - \rho c^2\left(1 - b_m^2\right)\right] & -\frac{N_y}{h}b_m^2 + \frac{N_x}{h} + \rho c^2 \\ +\frac{5}{6}\left(c_{55} - c_{44}b_m^2\right) + \frac{N_y}{h}b_m^2 - \frac{N_x}{h} - \rho c^2 & \\ -\frac{20}{\pi^3}\left(e_{15} - e_{24}b_m^2\right) + \frac{2\left(\pi^2 - 10\right)}{\pi^3}\left(e_{31} - e_{32}b_m^2\right) & -\frac{2}{\pi}\left(e_{31} - e_{32}b_m^2\right) \end{vmatrix}$$

Appendix B

The expressions of A_n, B_n, D_n and F_n related to the amplitude ratios α_n, β_n and χ_n are given by

$$A_n = \begin{vmatrix} \frac{\eta^2}{12}\left(b_n^2c_{22} - c_{66} + \rho c^2 - \frac{12c_{44}}{\eta^2}\right) & -\frac{\eta^2}{12}\left[b_n^3c_{22} - b_n\left(c_{12} + 2c_{66}\right) - b_n\rho c^2\right] & \frac{2b_n}{\pi}\left(e_{32} + e_{24}\right) \\ \frac{\eta^2}{12}\left[b_n^3c_{22} - b_n\left(c_{12} + 2c_{66}\right) - b_n\rho c^2\right] & -\frac{\eta^2}{12}\begin{bmatrix} c_{11} - 2b_n^2\left(c_{12} + 2c_{66}\right) + b_n^4c_{22} - \frac{12}{\eta^2}\rho c^2 \\ -\frac{12}{\eta^2 h}\left(N_x - b_n^2N_y\right) - \rho c^2\left(1 - b_n^2\right) \end{bmatrix} & -\frac{2}{\pi}\left(e_{31} - b_n^2e_{32}\right) \\ \frac{2b_n}{\pi}\left(e_{24} + e_{32}\right) & \frac{2}{\pi}\left(e_{31} - b_n^2e_{32}\right) & -\frac{1}{2}\left(\kappa_{11} - b_n^2\kappa_{22} + \frac{\pi^2\kappa_{33}}{\eta^2}\right) \end{vmatrix}$$

$$B_n = \begin{vmatrix} -\frac{\eta^2 b_n}{12}\left(c_{12} + c_{66}\right) & -\frac{\eta^2}{12}\left[b_n^3c_{22} - b_n\left(c_{12} + 2c_{66}\right) - b_n\rho c^2\right] & \frac{2b_n}{\pi}\left(e_{32} + e_{24}\right) \\ -\frac{\eta^2}{12}\left[-c_{11} + b_n^2\left(c_{12} + 2c_{66}\right) - \rho c^2\right] & -\frac{\eta^2}{12}\begin{bmatrix} c_{11} - b_n^2\left(2c_{12} + 4c_{66}\right) + b_n^4c_{22} - \frac{12}{\eta^2}\rho c^2 \\ -\frac{12}{\eta^2 h}\left(N_x - b_n^2N_y\right) - \rho c^2\left(1 - b_n^2\right) \end{bmatrix} & -\frac{2}{\pi}\left(e_{31} - b_n^2e_{32}\right) \\ -\frac{2}{\pi}\left(e_{15} + e_{31}\right) & \frac{2}{\pi}\left(e_{31} - b_n^2e_{32}\right) & -\frac{1}{2}\left(\kappa_{11} - b_n^2\kappa_{22} + \frac{\pi^2\kappa_{33}}{\eta^2}\right) \end{vmatrix}$$

$$D_n = \begin{vmatrix} \frac{\eta^2}{12}\left(b_nc_{22} - c_{66} + \rho c^2 - \frac{12c_{44}}{\eta^2}\right) & -\frac{\eta^2 b_n}{12}\left(c_{12} + c_{66}\right) & \frac{2b_n}{\pi}\left(e_{32} + e_{24}\right) \\ \frac{\eta^2}{12}\left[b_n^3c_{22} - b_n\left(c_{12} + 2c_{66}\right) - b_n\rho c^2\right] & -\frac{\eta^2}{12}\left[-c_{11} + b_n^2\left(c_{12} + 2c_{66}\right) - \rho c^2\right] & -\frac{2}{\pi}\left(e_{31} - b_n^2e_{32}\right) \\ \frac{2b_n}{\pi}\left(e_{24} + e_{32}\right) & -\frac{2}{\pi}\left(e_{15} + e_{31}\right) & -\frac{1}{2}\left(\kappa_{11} - b_n^2\kappa_{22} + \frac{\pi^2\kappa_{33}}{\eta^2}\right) \end{vmatrix}$$

$$F_n = \begin{vmatrix} \frac{\eta^2}{12}\left(b_nc_{22} - c_{66} + \rho c^2 - \frac{12c_{44}}{\eta^2}\right) & -\frac{\eta^2}{12}\left[b_n^3c_{22} - b_n\left(c_{12} + 2c_{66}\right) - b_n\rho c^2\right] & -\frac{\eta^2 b_n}{12}\left(c_{12} + c_{66}\right) \\ \frac{\eta^4}{12}\left[b_n^3c_{22} - b\left(c_{12} + 2c_{66}\right) - b_n\rho c^2\right] & -\frac{\eta^4}{12}\begin{bmatrix} c_{11} - b_n^2\left(2c_{12} + 4c_{66}\right) + b_n^4c_{22} - \frac{12}{\eta^2}\rho c^2 \\ -\frac{12}{\eta^2 h}\left(N_x - b_n^2N_y\right) - \rho c^2\left(1 - b_n^2\right) \end{bmatrix} & -\frac{\eta^4}{12}\left[-c_{11} + b_n^2\left(c_{12} + 2c_{66}\right) - \rho c^2\right] \\ \frac{2b_n}{\pi}\left(e_{24} + e_{32}\right) & \frac{2}{\pi}\left(e_{31} - b_n^2e_{32}\right) & -\frac{2}{\pi}\left(e_{15} + e_{31}\right) \end{vmatrix}$$